Available online at www.sciencedirect.com
ScienceDirect
Journal of Sound and Vibration 317 (2008) 646–656
JOURNAL OF SOUND AND VIBRATION
www.elsevier.com/locate/jsvi

Distinguishing between the interior pressures induced by independent sources within a room using the probabilistic approach and model class selection index: An experiment

Y.Y. Lee*, H.F. Lam, H.Y. Sun

Department of Building and Construction, City University of Hong Kong, Tatchee Avenue, Hong Kong Special Administrative Region, Kowloon Tong, Kowloon, Hong Kong, China

Received 10 May 2007; received in revised form 15 February 2008; accepted 30 March 2008
Handling Editor: L.G. Tham
Available online 6 June 2008

Abstract

This study presents the first full-scale experiment to verify the effectiveness of the probabilistic approach to distinguish between the interior pressures that are induced from independent sources within a room. This study furthers the theoretical work of a companion paper in which no experimental verification was conducted and the number of interior sources was assumed to be known in the parameter identification process. The two main contributions of this paper are (1) the development of a model class selection index that can indicate the number of interior sources and (2) the experimental verification of the probabilistic approach.

1. Introduction

Interior acoustics is very important for all big cities, including Hong Kong, because they have many noise problems. Acoustic experts are required to distinguish the independent noise sources to determine whether the noise that is generated by a particular machine exceeds an established limit in order to design suitable mitigation measures for each noise source. There is no well-established method to solve this acoustic problem. The companion paper [1] introduced a theoretical model that uses the probabilistic approach to distinguish between the interior pressures, which are induced from independent sources within a room, but no experiment was conducted to prove its validity. One drawback of the study [1] is that the number of interior sources was assumed to be given in the parameter identification process, or, the idea of a model class selection was not adopted. Lee et al. [2] recently presented a theoretical simulation to identify the sound leakages on a wall of an enclosed room using the same probabilistic approach. Similar to that of Ref. [1], the drawback of their study was that the number of leakages was assumed to be known in the parameter identification process.

*Corresponding author. Tel.: +852 2788 9847; fax: +852 2788 7612.
E-mail address: bcraylee@cityu.edu.hk (Y.Y. Lee).

0022-460X/$ - see front matter
doi:10.1016/j.jsv.2008.03.053

Although probabilistic analysis has been in use for a long time, the Bayesian method for model comparison has only recently been developed in depth. This is referred to as model class selection in the literature. In 1992, Mackay [3] was the first to investigate the Bayesian approach to regularization and model comparison (model class selection) and used the inference problem of interpolating noisy data. In his study, models were ranked by evaluating the evidence, a solely data-dependent measure that intuitively and consistently combines a model's ability to fit the data with its complexity. Recently, Beck and Yuen [4] presented a Bayesian probabilistic approach for selecting the most plausible class of models for a structural or mechanical system within a specified set of model classes, based on system response data. The basis of the approach is to rank the classes of models based on their probabilities conditional on the response data that can be calculated based on Bayes' theorem and an asymptotic expansion of the evidence for each model class. The two aforementioned approaches are mainly used for system identification in structural engineering, and have never been applied to interior acoustic problems. This paper introduces a probabilistic system identification method combined with model class selection to solve interior acoustic problems.

2. Theory

2.1. Acoustic model

The acoustic models in the companion paper [1] and other Refs. [5–7] consider only rectangular rooms. Hence, this paper considers practical and non-rectangular cases. The complex acoustic pressure $p(x, y, z)$ within a non-rectangular room is described by the frequency domain acoustic wave equation [8]

$$(\nabla^2 + k^2)p(x,y,z) = -\mathrm{j}\rho_0\omega q(x_0,y_0,z_0), \tag{1}$$

where k and ω are the wavenumber and angular velocity of the sound waves, $\mathrm{j} = \sqrt{-1}$, ρ_0 the air density, and $p(x, y, z)$ the acoustic pressure at the position of (x, y, z) in the Cartesian coordinates, as shown in Fig. 1. Note that if $a = 0$ and $b = L_y$, the model is rectangular. $q(x_0, y_0, z_0)$ is the source strength at (x_0, y_0, z_0), which describes the volume velocity per unit volume.

If the acoustic pressure field is described by the trial solution $\hat{p}(x,y,z)$, the residual of Eq. (1) can be defined as

$$R(\hat{p}(x,y,z)) = (\nabla^2 + k^2)\hat{p}(x,y,z) + \mathrm{j}\rho_0\omega q(x_0,y_0,z_0). \tag{2}$$

A set of shape functions $\phi_J(x,y,z)$, where $J = 1,2,\ldots,\bar{J}$ may now be selected to represent the spatial variation of the pressure field. The trial solution is expressed as

$$\hat{p}(x,y,z) = \sum_{J=1}^{\bar{J}} P_J\phi_J(x,y,z), \tag{3}$$

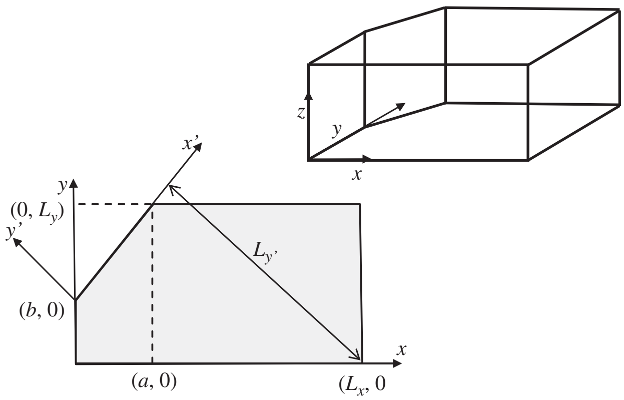

Fig. 1. Iso view and top view of a non-rectangular room.

where $\phi_J(x,y,z)$ is the Jth shape function that satisfies the geometrical boundary conditions (see Eqs. (4a)–(4d)), P_J is the unknown modal amplitude of the Jth shape function, and $\bar{J}$ is the number of modes that retained in the modal decomposition:

$$\left.\frac{\partial\phi}{\partial x}\right|_{x=0,0\leqslant y\leqslant b} = \left.\frac{\partial\phi}{\partial x}\right|_{x=Lx} = 0; \quad \left.\frac{\partial\phi}{\partial y}\right|_{y=0} = \left.\frac{\partial\phi}{\partial y}\right|_{y=Ly,a\leqslant x\leqslant Lx} = 0 \tag{4a,b}$$

$$\left.\frac{\partial\phi}{\partial z}\right|_{z=0} = \left.\frac{\partial\phi}{\partial z}\right|_{z=Lz} = 0; \quad \left.\frac{\partial\phi}{\partial y'}\right|_{0\leqslant x\leqslant a,b\leqslant y\leqslant Ly} = 0, \tag{4c,d}$$

where (x', y') are the local coordinates in Fig. 1:

$$\phi_J = \cos\frac{l\pi x}{L_x}\cos\frac{m\pi y}{L_y}\cos\frac{n\pi z}{L_z}\cos\frac{l'\pi(a(y-b)-(L_y-b)x)}{(L_x-a)(L_y-b)+aL_y} \tag{4e}$$

where l, m, n, and l are integers. ϕ_J is a function that can satisfy the boundary conditions in Eqs. (4a)–(4d).

Using the Galerkin approach [5], the weighted residual in Eq. (2) is set to zero:

$$\int_V \phi_J R(\hat{p}(x,y,z))\,\mathrm{d}v = 0 \tag{5a}$$

or

$$\int_V \phi_J \nabla^2\hat{p}\,\mathrm{d}v + k^2\int_V \phi_J\hat{p}\,\mathrm{d}v + \mathrm{j}\rho_0\omega\int_V \phi_J q\,\mathrm{d}v = 0. \tag{5b}$$

According to the gradient theorem [5], the first term on the left-hand side of Eq. (5b) can be expressed as

$$\int_V \phi_J\nabla^2\hat{p}\,\mathrm{d}v = \int_V \hat{p}\nabla^2\phi_J\,\mathrm{d}v + \int_A \phi_J\frac{\partial\hat{p}}{\partial n}\,\mathrm{d}s - \int_A \frac{\partial\phi_J}{\partial n}\hat{p}\,\mathrm{d}s, \tag{6}$$

where V and A represent the volume and the surface area of the room.

Substituting Eq. (6) into Eq. (5b) gives

$$\int_V \hat{p}\nabla^2\phi_J\,\mathrm{d}v + \int_A \phi_J\frac{\partial\hat{p}}{\partial n}\,\mathrm{d}s - \int_A \frac{\partial\phi_I}{\partial n}\hat{p}\,\mathrm{d}s + k^2\int_V \phi_J\hat{p}\,\mathrm{d}v + \mathrm{j}\rho_0\omega\int_V \phi_J q\,\mathrm{d}v = 0. \tag{7}$$

From Eq. (7), $\bar{J}$ equations can be set up for $J = 1$ to $\bar{J}$, and used for solving the $\bar{J}$ unknown modal amplitude P_J in Eq. (3). Then, the corresponding sound pressure in the time domain can be derived using the inverse Fourier transform method [9]. If $\bar{K}$ point sound sources exist within the room, the last term in Eq. (7) can be given by

$$\mathrm{j}\rho_0\omega\int_V \phi_I q\,\mathrm{d}v = \mathrm{j}\rho_0\omega\sum_{K=1}^{\bar{K}} Q_K\phi_J(x_K, y_K, z_K), \tag{8}$$

where (x_K, y_K, z_K) is the coordinate of the Kth sound sources, and Q_K is the source strengths. Note that by setting the source strength equal to zero, the solution of Eq. (7) is a set of eigenvalues representing the cavity resonant frequencies.

The sound pressure level in dB scale that is due to the Kth source at a particular measurement location is defined by

$$\mathrm{SPL}_K = 10\log\left(\frac{\hat{p}_K(x,y,z)}{p_{\mathrm{ref}}}\right)^2, \tag{9}$$

where p_{ref} is the reference pressure $= 2\times10^{-5}$ Pa.

2.2. Bayesian approach

The proposed probabilistic approach, which was originally employed in structural model updating and damage detection, was recently employed in Refs. [1,2] for system identification of interior acoustic problems.

The probabilistic approach is briefly described as follows. We define $\boldsymbol{\theta} = \{\mathbf{a}^{\mathrm{T}}\sigma\}^{\mathrm{T}}$ as the uncertain parameter vector to be updated, where $\mathbf{a}$ contains the sound source strength and the modal vibration amplitudes, and σ represents the prediction error and it is the uncertain parameter of the probabilistic model $\boldsymbol{\theta} \in S(\boldsymbol{\theta}) \subseteq R^{N_{\mathbf{a}}+1}$, where $N_{\mathbf{a}}$ is the dimension of the uncertain parameter vector $\mathbf{a}$. The posterior marginal probability density function (PDF) of the unknown parameters $\mathbf{a}$ can be given by

$$\pi(\mathbf{a}|D_N, M_{\bar{K}}) = \int_0^{\infty} c\pi(D_N|\mathbf{a}, \sigma, M_{\bar{K}})\,\mathrm{d}\sigma, \tag{10}$$

where D_N is the set of measured sound pressure data, $M_{\bar{K}}$ the acoustic model that is described in the previous section, and c the normalizing constant. The term $\pi(D_N|\mathbf{a}, \sigma, M_{\bar{K}})$ in Eq. (10) is given by

$$\pi(D_N|\mathbf{a}, \sigma, M_{\bar{K}}) = \frac{1}{(\sqrt{2\pi}\sigma)^{NN_O}} \exp\left[-\frac{1}{2\sigma^2}\sum_{\tau=1}^{N} ||\hat{p}(\tau) - p(\tau;\mathbf{a})||^2\right], \tag{11}$$

where N_O is the number of measurement stations, N the number of measured time steps at each measurement location, (τ) the vector of measured sound pressures at the τth time step, $p(\tau;\mathbf{a})$ the vector of calculated sound pressures that is based on the model M_K for the given set of uncertain parameters $\mathbf{a}$, and $||\cdot||$ the usual Euclidean norm of a vector.

Hence, the posterior PDF for a particular uncertain parameter $\boldsymbol{a}^*$ is given by

$$\pi(\boldsymbol{a}^*|D_N, M_{\bar{K}}) = \int_{S(\mathbf{a}')} \pi(\mathbf{a}|D_N, M_{\bar{K}})\,\mathrm{d}\mathbf{a}', \tag{12}$$

where $\mathbf{a}'$ is the uncertain parameter vector that excludes $\boldsymbol{a}^*$, and $S(\mathbf{a}')$ is the predefined domain of $\mathbf{a}'$.

Model updating problems in such situations can be classified as identifiable cases [10,11]. When the number N is not large or the location of the measurement station is not informative, it is possible for model updating problems to fall into the category of unidentifiable cases. It must be pointed out that the treatment of model updating problems in unidentifiable cases is much more complex than that in identifiable cases.

2.3. Model class selection index

In Bayesian system identification, one aims not only to identify the values of the uncertainties in the model, but also to find the best (optimal) model in a specified class of models [4,12]. The number of parameters may not be certain and is also predicted or identified. In the current study, the number of point sources is unknown, which directly affects model class selection. Hence, a model class selection index is defined to evaluate a model class with $\bar{K}$ point sound sources:

$$I_{\bar{K}} = \frac{\int_{S(\mathbf{a})} \pi(\mathbf{a}|\mathbf{D}_N, \mathbf{M}_{\bar{K}})\,\mathrm{d}\mathbf{a}}{S(\mathbf{a})}. \tag{13}$$

The index in Eq. (13) is defined proportional to the integration of the PDF with respect to the uncertain parameters, and normalized so that the maximum value is equal to one. It can be seen that a higher index value implies a higher probability of the number of sources equal to $\bar{K}$.

3. Experiment

The acoustic experiment was carried out in Hong Kong in the laboratory of Acoustics and Air Testing Laboratory Co. Ltd. The experimental setup is shown in Fig. 2. Experimental cases of one and two sound sources were carried out. Two loudspeakers, S1 and S2, were employed and set at (3.39, 2.79, and 0.335 m) and (2.69, 1.6, and 0.3875 m), respectively. Note that (1) S2 was off for the case of one source and (2) when the sound contribution from one of the two loudspeakers to a particular location was measured in the case of two sources, the other loudspeaker was off. Two microphones (B&K type 4188), M1 and M2, to measure the acoustic responses were placed at (4.79, 1.0, and 1.04 m) and (4.79, 2.19, and 0.90 m), respectively. The walls, floor, and ceiling of the room are acoustically rigid. Random white noise signals that were the input data in the

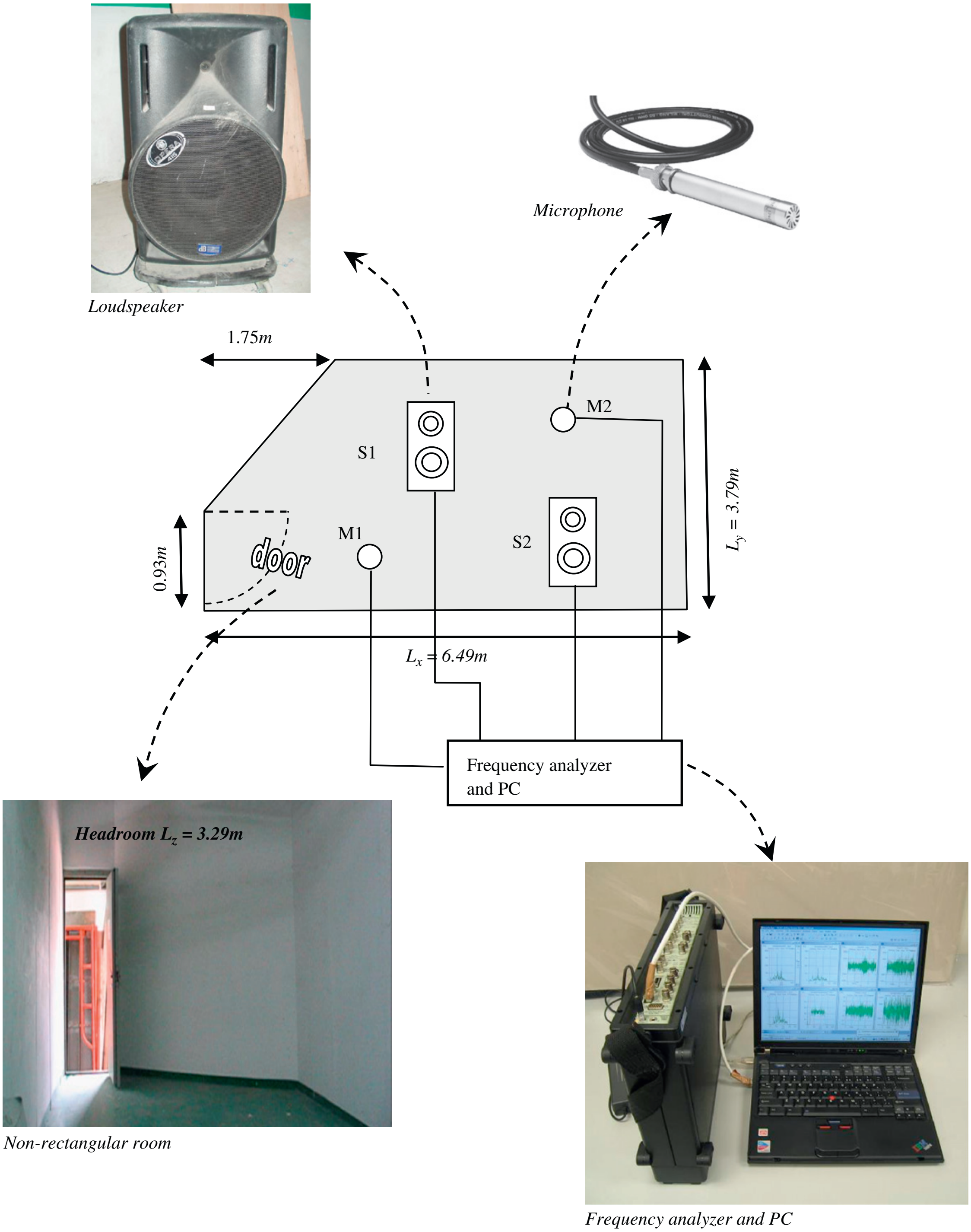

Fig. 2. Setup of the full-scale experiment.

system identification process and generated by a multianalyzer system (PULSE^{TM} type 3560c) were input into loudspeakers S1 and S2, and monitored by a PC. The lower and upper cut-off frequencies of the loudspeakers were 65 and 115 Hz, respectively. Sound signals of 2 s that were measured by the microphones at a time step of

0.9766 ms were recorded via the PULSE software, and stored on the PC. Photos of the loudspeaker, PC, frequency analyzer, microphone, and enclosed room can be found in Fig. 2.

4. Results

Tables 1a and b show the identification results in the experimental cases of one and two sound sources. The first 64 acoustic modes are considered in the Bayesian models. The non-zero acoustic resonant frequencies of the first and last modes are 26.4 and 114.2 Hz. Figs. 3a and b show the mode convergence studies of the cases that are marked with "+" in Table 1b. It can be seen that a reasonably convergent solution of the uncertain parameters can be obtained using at least the first 64 acoustic modes in the Bayesian model. As the number of sound sources is unknown in the identification process, the identification results from the models that consider different numbers of sound sources are evaluated. As the source strengths (flow volume per second) could not be measured accurately in the experiment, they are not shown in Tables 1a and 1b. The models with the correct number of sources give reasonably accurate identifications of the uncertain parameters. The maximum distance error is 0.57 that is acceptable when considering the room dimensions of $6.49\,\mathrm{m} \times 3.79\,\mathrm{m} \times 3.29\,\mathrm{m}$. The PDFs of the uncertain parameters show a crisp peak within the domain that is considered (see Figs. 4a and b and 5c–e). The PDFs are obtained from Eq. (12). The optimal parameter values are the values of highest

Table 1a
Identification results of the one-source experiment

True values $(S_{1x}, S_{1y}, S_{1z}) = (3.39, 2.79, 0.335)\,\mathrm{m}$			
No. of sound sources considered in the acoustic model	Three sound sources	Two sound sources	One sound source
Identified values			
(Q_1, Q_2, Q_3) ($\times 10^{-3}\,\mathrm{m}^3/\mathrm{s}$)	(2.6619, 0.0424, 0.001)	(2.7408, −0.4838, N/A)[c]	(2.6926, N/A, N/A)[a]
(S_{1x}, S_{1y}, S_{1z}) (m)	(3.6082, 2.5072, 0.5308)	(3.6386, 2.5587, 0.5144)[d]	(3.6703, 2.5090, 0.3597)[b]
(S_{2x}, S_{2y}, S_{2z}) (m)	Unidentifiable	Unidentifiable[e]	N/A
(S_{3x}, S_{3y}, S_{3z}) (m)	Unidentifiable	N/A	N/A
Distance error			
(S_{1x}, S_{1y}, S_{1z}) (m)	0.41	0.38	0.40

[a–e]See Figs. 4a–e for the corresponding normalized PDFs.

Table 1b
Identification results of the two-source experiment

True values $(S_{1x}, S_{1y}, S_{1z}) = (3.39, 2.79, 0.335)\,\mathrm{m}$; $(S_{1x}, S_{1y}, S_{1z}) = (2.69, 1.60, 0.3875)\,\mathrm{m}$			
No. of sound sources considered in the acoustic model	Three sound sources	Two sound sources	One sound source
Identified values			
(Q_1, Q_2, Q_3) ($\times 10^{-3}\,\mathrm{m}^3/\mathrm{s}$)	(2.7195, 1.7518, 0.073)	(2.6734, 1.8131, N/A)[c,f]	(3.1107, N/A, N/A)[a]
(S_{1x}, S_{1y}, S_{1z}) (m)	(3.4874, 3.3262, 0.5468)	(3.4918, 3.1384, 0.5415)[d,f]	Unidentifiable[b]
(S_{2x}, S_{2y}, S_{2z}) (m)	(2.3256, 1.3324, 0.5141)	(2.2132, 1.3015, 0.4961)[e,f]	N/A
(S_{3x}, S_{3y}, S_{3z}) (m)	Unidentifiable	N/A	N/A
Distance error			
(S_{1x}, S_{1y}, S_{1z}) (m)	0.58	0.42	N/A
(S_{2x}, S_{2y}, S_{2z}) (m)	0.55	0.57	N/A

[a–e]See Figs. 5a–e for the normalized PDFs.
[f]See Figs. 3a and b for the convergences.

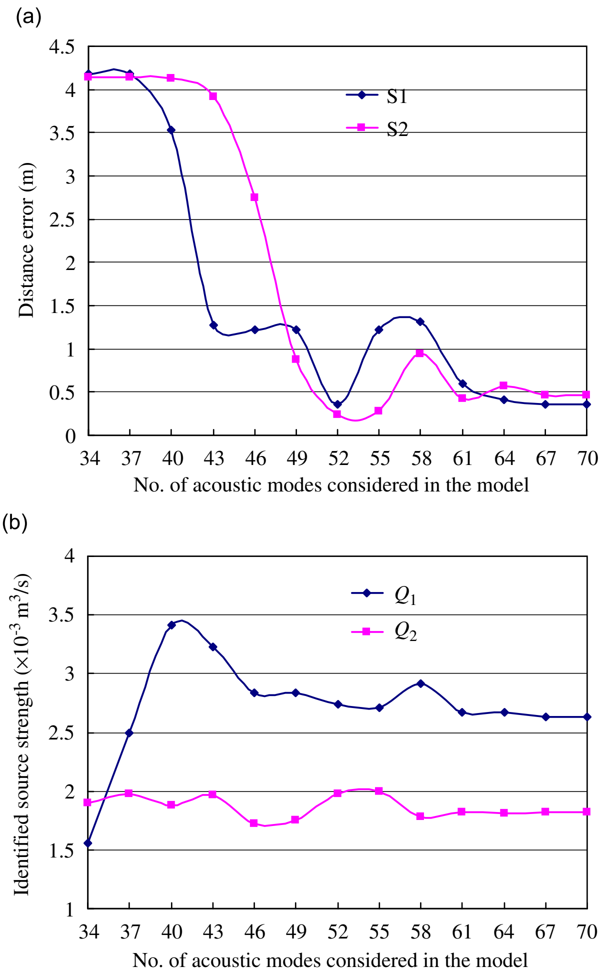

Fig. 3. (a) Distance errors of the source locations vs. the number of model input acoustic modes. (b) Identified source strength vs. the number of model input acoustic modes.

probability density. Note that to present the three-dimensional plots, only two independent variables are selected (i.e., S_x and S_y). The models in which the numbers of sound sources are larger than the true values can give reasonable predictions of the true sound source locations. The locations of the inexistent sound sources are unidentifiable due to modeling error (see Fig. 4e for the PDF of the case that is marked with "e" in Table 1a). No peak can be found in the PDF plot of the inexistent source locations within the domain that is considered. The other uncertain parameters, such as source strengths and existent source locations, are all identifiable, and their corresponding PDFs show a crisp peak within the domain that is considered (see Figs. 4c and d). The maximum distance error of these models is 0.58 m, which is close to that of the models with the correct number of sources. The model in which the number of sound sources is smaller than the true value cannot crisply identify the sound location and gives an unidentifiable result, according to the definition in Ref. [10]. In Fig. 5b, two peaks are found on the PDF, which is different from the nearly flat surface of the other unidentifiable case in Fig. 4e. The other uncertain parameter (i.e., source strength) is identifiable, and its corresponding PDF in Fig. 5a shows a crisp peak within the domain that is considered. In general, the distance error in the two-source experiment is larger than that in the one-source experiment due to the greater number of parameters that are considered in the identification process.

According to Refs. [1,2], unidentifiable cases can occur due to several factors, such as measurement noise, modal truncation, and measurement on a nodal line. Therefore, it is not possible to conclude that the number of sound sources that is employed in the identification process is wrong when the results of updating are

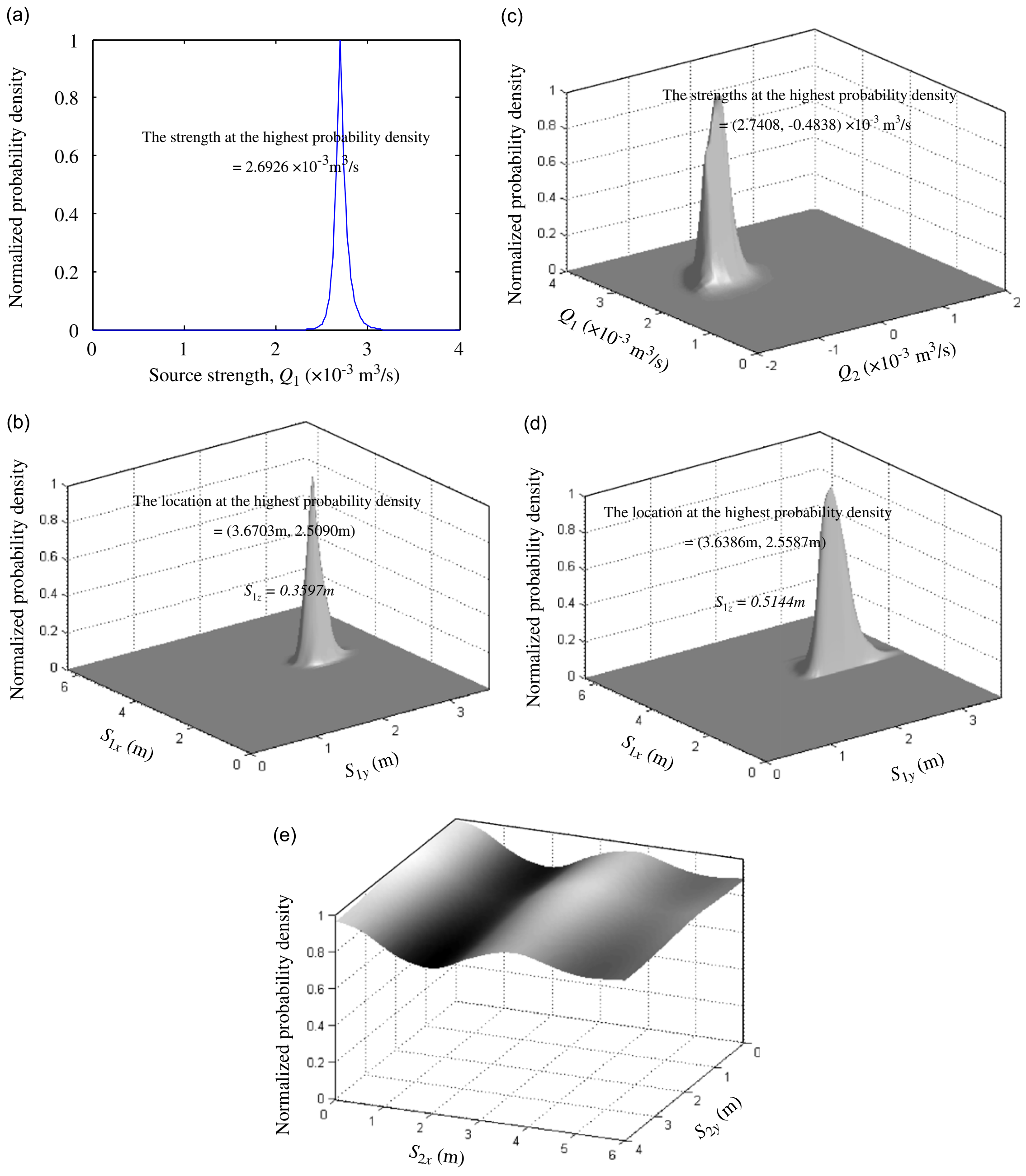

Fig. 4. (a) Normalized probability density vs. the source strength (one source in the experiment, one source in the model). (b) Normalized probability density vs. the source location (one source in the experiment, one source in the model). (c) Normalized probability density vs. the source strengths (one source in the experiment, two sources in the model). (d) Normalized probability density vs. the first source location (one source in the experiment, two sources in the model). (e) Normalized probability density vs. the second source location (one source in experiment, two sources in the model).

unidentifiable. Thus, the newly developed model class selection index in Eq. (13) is extremely important in selecting the best model class based on the set of experimental data to identify the number of sound sources. Figs. 6a and b clearly show that the index values of the one- and two-source model classes are the highest in

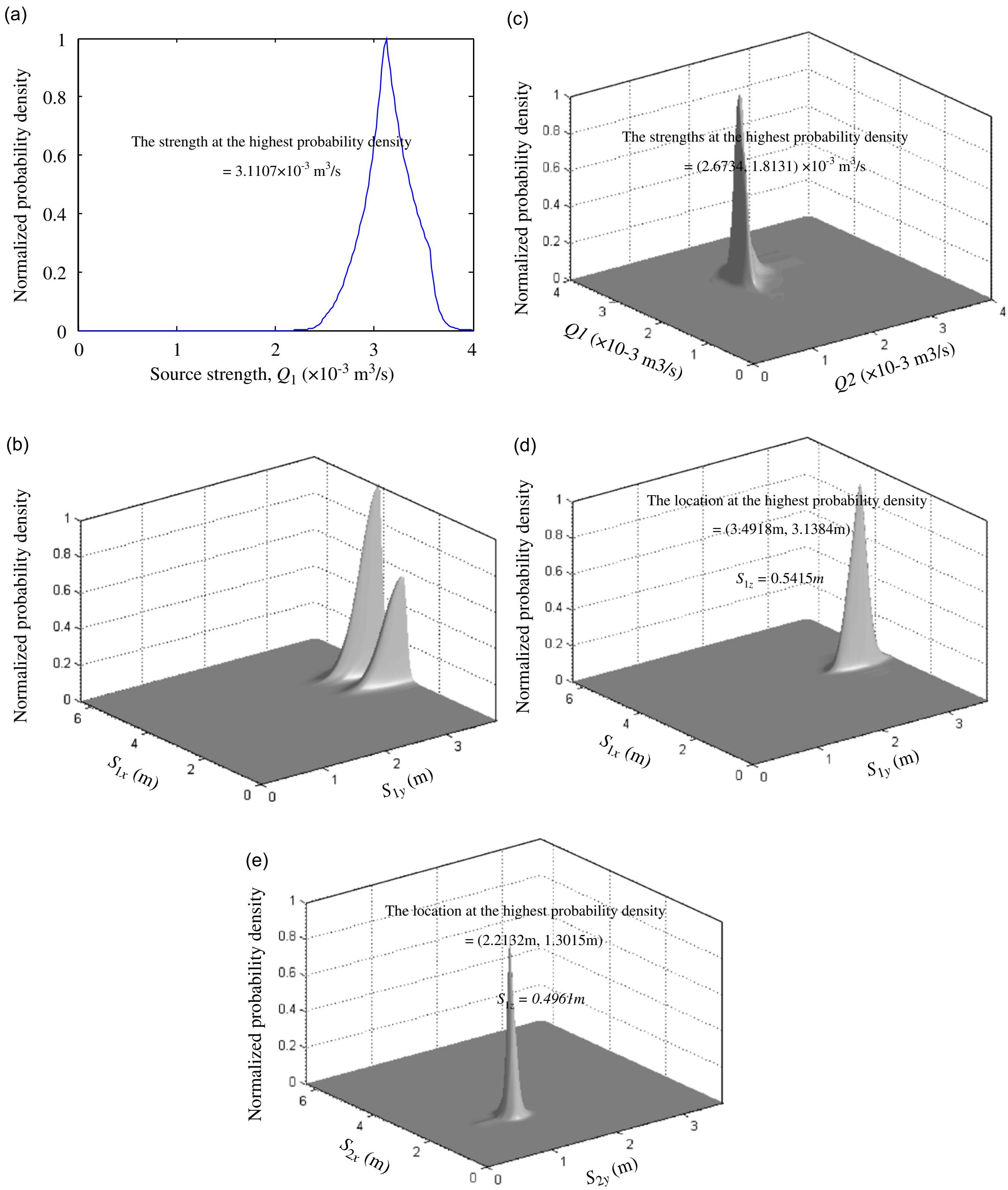

Fig. 5. (a) Normalized probability density vs. the source strength (two sources in the experiment, one source in the model). (b) Normalized probability density vs. the source location (two sources in the experiment, one source in the model). (c) Normalized probability density vs. the source strengths (two sources in the experiment, two sources in the model). (d) Normalized probability density vs. the first source location (two sources in the experiment, two sources in the model). (e) Normalized probability density vs. the second source location (two sources in the experiment, two sources in the model).

the experimental cases of one and two sources, respectively. The model class with the highest index is the best model class based on the set of experimental data, and its corresponding number of sound sources is defined in the proposed method as the true number. The experimental verification clearly shows that the index that is

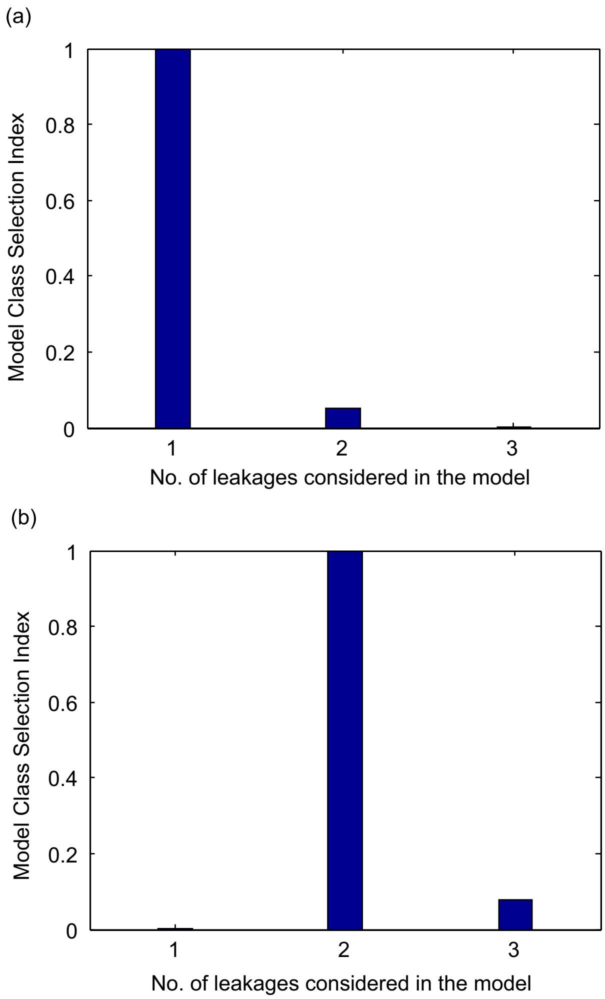

Fig. 6. Model class selection index (a) one-source experiment; (b) two-source experiment.

Table 2
Sound pressure contributions (two sound sources)

	From S_1 (dB)	From S_2 (dB)	Total (dB)
At M_1			
True value	88.0	83.4	88.9
Predicted	86.9	83.8	88.3
At M_2			
True value	90.3	85.4	91.2
Predicted	89.2	84.4	90.3

defined in Eq. (13), which is the main contribution of this study, is a valid indicator for identifying the number of sound sources. Based on the results in Fig. 6b, the Bayesian model with two sound sources is used for distinguishing between the sound pressure levels in the case of two sound sources. Table 2 shows a comparison between the identified and true sound pressure levels that are contributed by the two sound sources. The Bayesian identifications agree reasonably with the measurements at the two locations.

5. Conclusions

This study presented experimental verification of the effectiveness of the application of the proposed probabilistic method to sound contribution identification. The identification results of the experiments in which the number of sound sources is unknown show that the model class selection index can be used to identify the model class that best fits the measured data to identify the number of sound sources. With the aid of the model class selection index, the best Bayesian model is selected for the identification process. The uncertain model parameters of the selected model class are identifiable, and the predictions of the sound source contributions to a particular location are reasonably accurate.

6. Further work

The present probabilistic method is valid only for the interior acoustic problems that the noise sources are placed within the room. Further validations for other interior acoustic problems that the noise sources are placed outside the room are also very important. It is because there are many noise complaints in Hong Kong, in which the noise sources are exterior. It is expected that the successful validations can show the present probabilistic method useful for solving more acoustic problems

Acknowledgment

The work that was described in this paper was fully supported by a grant from the Research Grants Council of the Hong Kong Special Administrative Region, China [Project no. 9040798, RGC Ref. no. CityU 1142/03E].

References

[1] H.Y. Sun, Y.Y. Lee, A.Y.T. Leung, C.F. Ng, Distinguishing between the interior pressures induced from two independent sources within a room using the probabilistic approach, *Applied Acoustics* 69 (2008) 496–505.
[2] Y.Y. Lee, A.Y.T. Leung, H.F. Lam, H.Y. Sun, Reconstruction of the interior sound pressure of a room using the probabilistic approach, *Journal of Sound and Vibration* 298 (4–5) (2006) 887–891.
[3] D.J.C. Mackay, Bayesian interpolation, *Neural Computation* 4 (3) (1992) 415–447.
[4] J.L. Beck, K.V. Yuen, Model selection using response measurements: Bayesian probabilistic approach, *Journal of Engineering Mechanics—ASCE* 130 (2) (2004) 192–203.
[5] J. Pan, S.J. Elliott, K.H. Baek, Analysis of low frequency acoustic response in a damped rectangular enclosure, *Journal of Sound and Vibration* 223 (4) (1999) 543–566.
[6] A.J. Pretlove, Forced vibration of a rectangular panel backed by a closed rectangular cavity, *Journal of Sound and Vibration* 3 (3) (1966) 252–261.
[7] E.H. Dowell, G.F. Gorman, D.A. Smith, Acoustoelasticity: general theory, acoustic natural modes and forced response to sinuoidal excitation, including comparisons with experiment, *Journal of Sound and Vibration* 52 (4) (1977) 519–542.
[8] F. Fahy, *Sound and Structural Vibration, Radiation, Transmission and Response*, Academic Press, London, Orlando, 1985.
[9] D.E. Newland, *An Introduction to Random Vibrations and Spectral Analysis*, second ed, Longman, London, 1984.
[10] H.F. Lam, Structural Model Updating and Health Monitoring in the Presence of Modeling Uncertainties, PhD Thesis, Department of Civil Engineering, Hong Kong University of Science and Technology, 1999.
[11] L.S. Katafygiotis, H.F. Lam, Tangential-projection algorithm for manifold representation in unidentifiable model updating problems, *Earthquake Engineering and Structural Dynamics* 31 (4) (2002) 791–812.
[12] M. Grigoriu, C. Cornell, D. Veneziano, Probabilistic modeling as decision making, *Journal of Engineering Mechanics—ASCE* 105 (4) (1979) 585–596.